ATLAS combinations, couplings and spin/CP

Richard Polifka
University of Toronto

Higgs Hunting 2015
31.7.2015 LAL Orsay

Outline

- ATLAS, LHC @ CERN
- channel inputs
- mass combination
- couplings
  - κ-framework
- spin CP

$N = L^{*}\sigma_{prod}{}^{*}Br$

- Large Hadron Collider, Geneva (CH) - 26.7km
  - collisions every 50 ns (20 MHz)
  - 1368 bunches ~10^{11} protons -> pile up
    - **up to 35 simultaneous interactions in one bunch crossing**
- **ATLAS** - 4π detector, 44x25m, 7000t

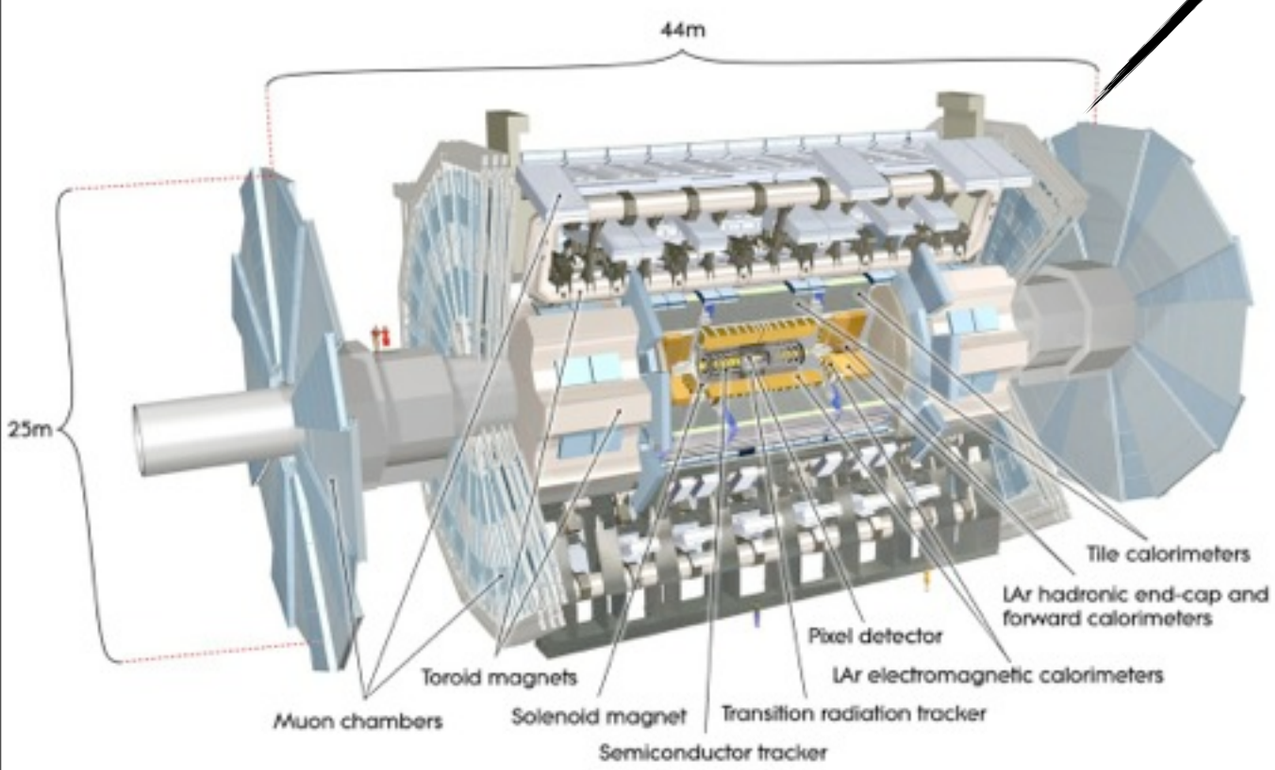

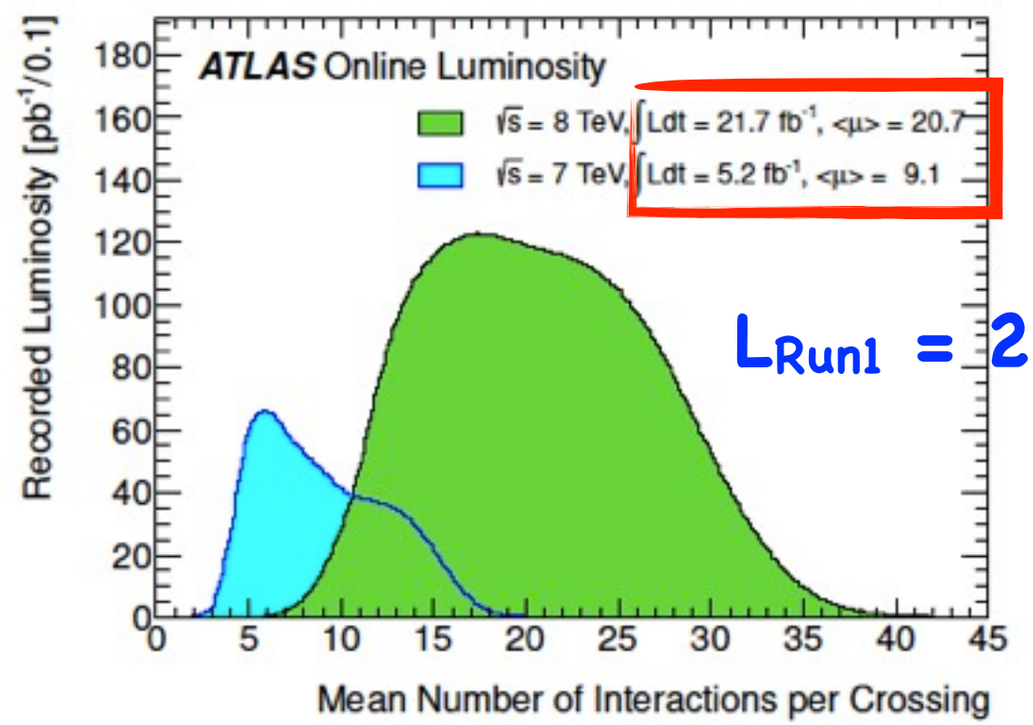

$L_{Run1} = 25\ fb^{-1}$

$N = L * \sigma_{prod} * Br$

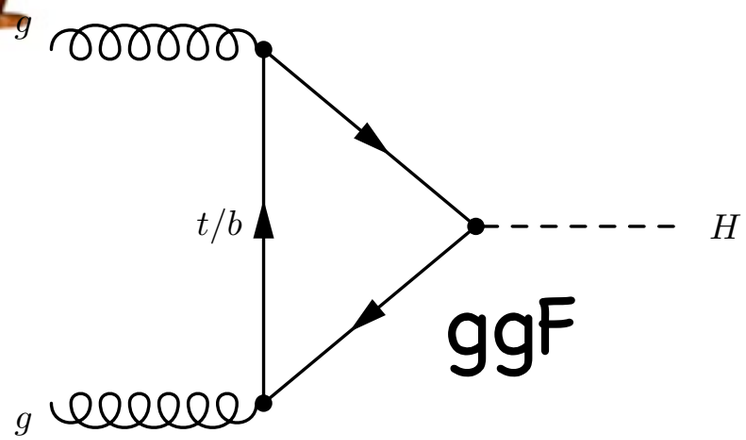

ggF

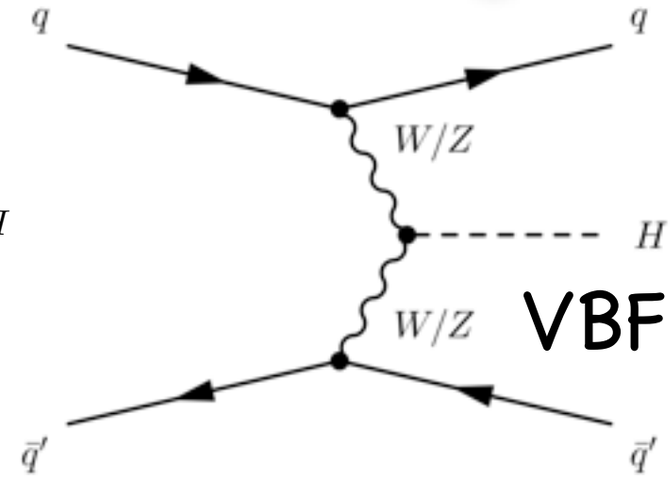

VBF

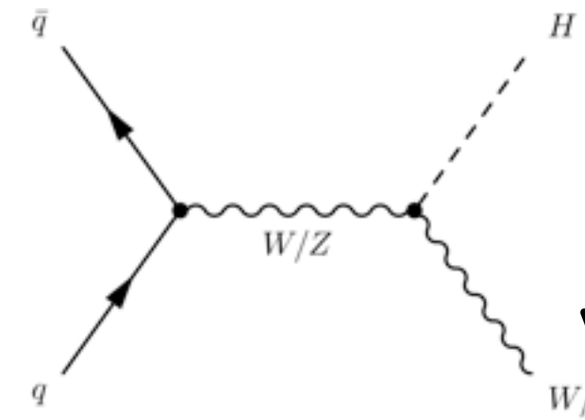

VH

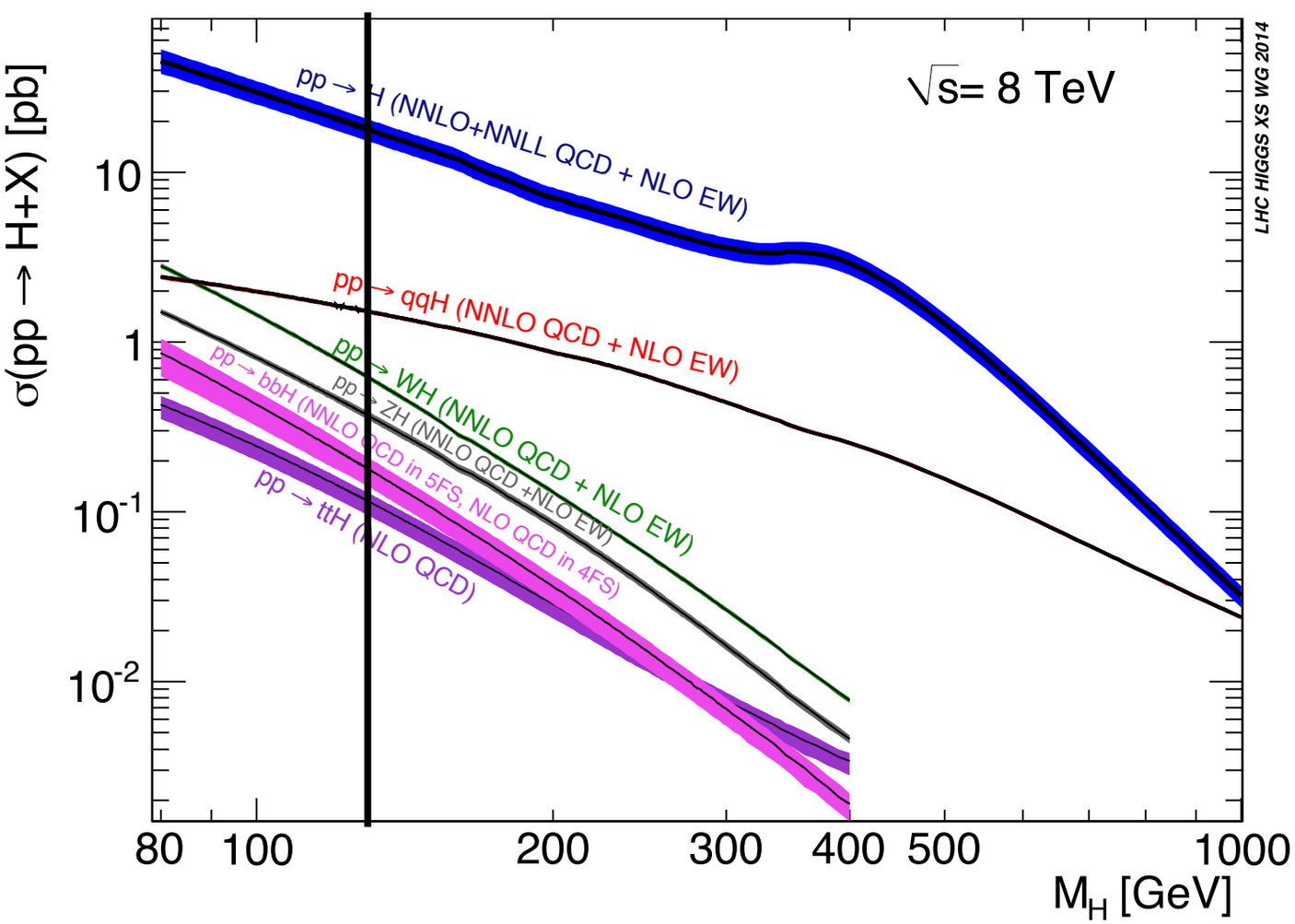

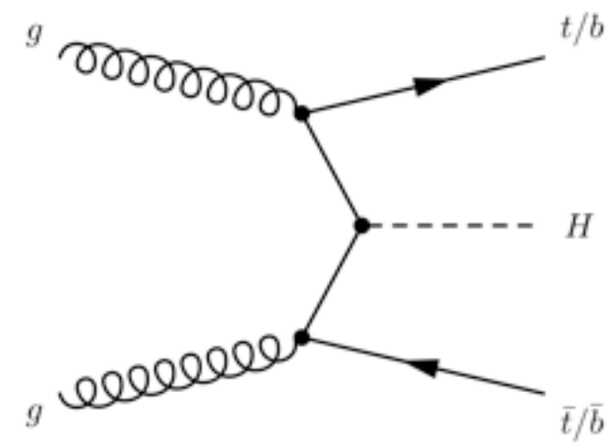

ttH

- measured modes:
  - gluon-gluon fusion (quark (top) loop) - ggF
  - vector boson fusion - VBF
  - vector boson associated production - VH, V=Z,W
  - ttbar associated production - ttH (direct top coupling)

$N = L^{*}\sigma_{prod}{}^{*}Br$

$$\mu = \frac{\sigma \times BR}{(\sigma \times BR)_{SM}}$$

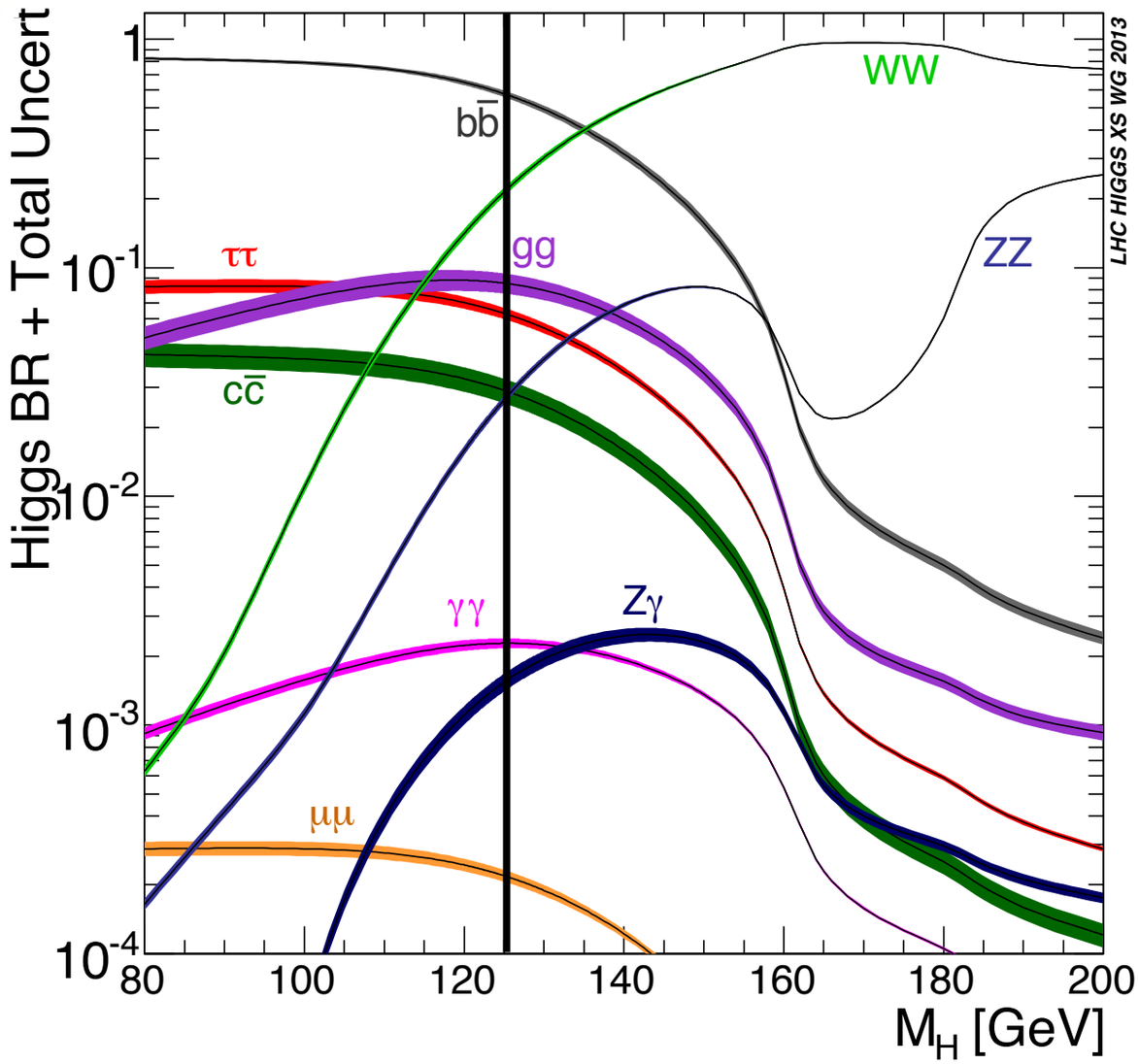

bb [%]	WW [%]	ττ [%]	ZZ [%]	γγ [%]	Zγ [%]	μμ [%]
56.9	22	6.2	3	0.2	0.16	0.022

arXiv:1507.04548

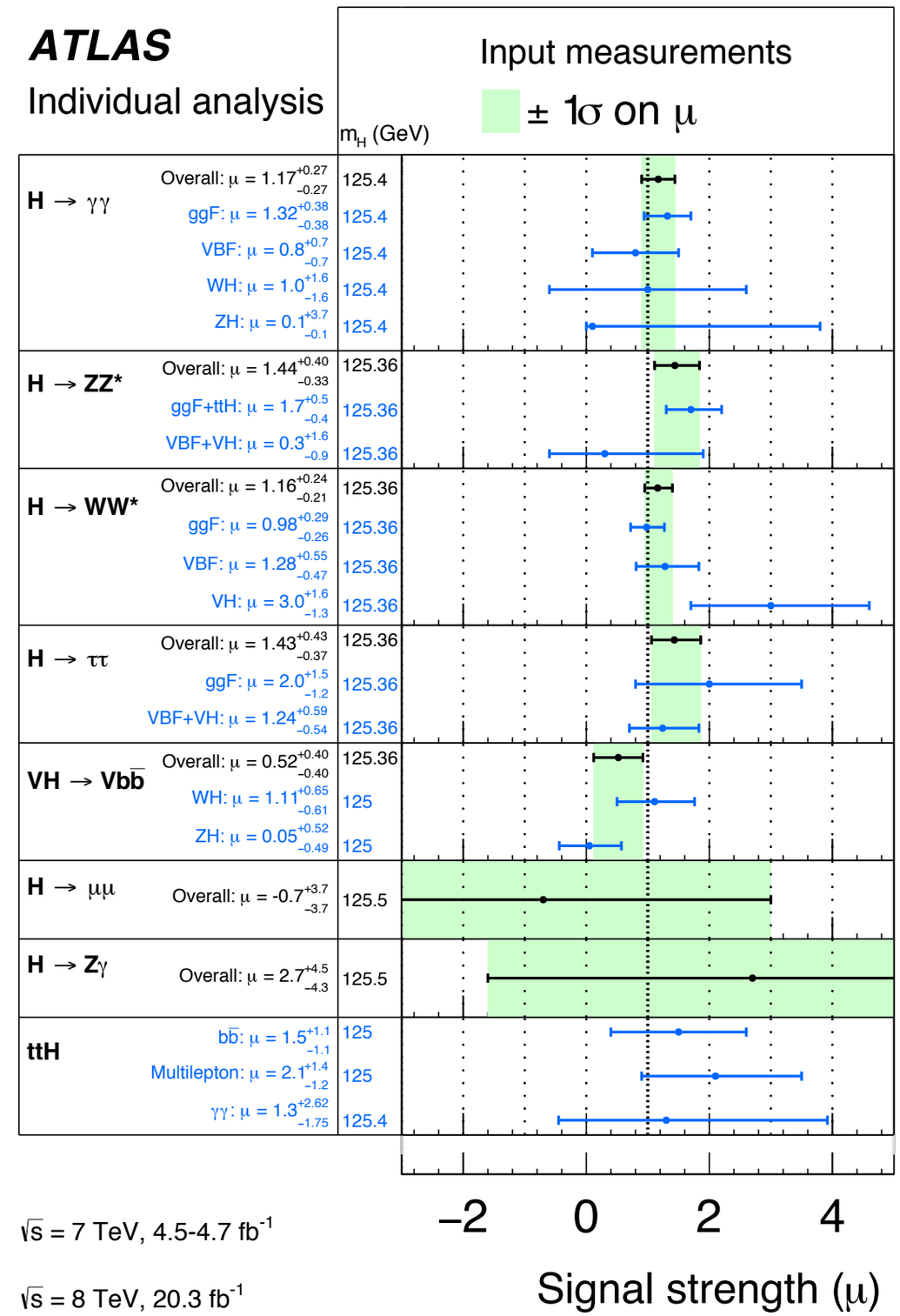

Combined mass

Phys. Rev. D. 90, 052004 (2014)

- H->ZZ and H->γγ channels
- H->γγ:
  - 10 categories
  - data fit:
    - Crystal Ball + exponential
- H->ZZ:
  - 4 categories (ee, μμ, eeμμ, μμee)

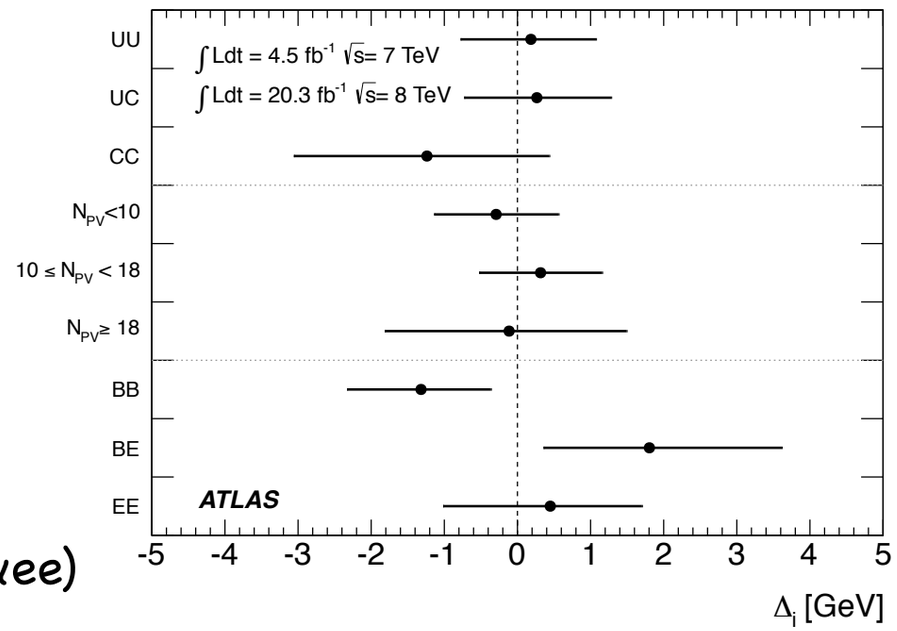

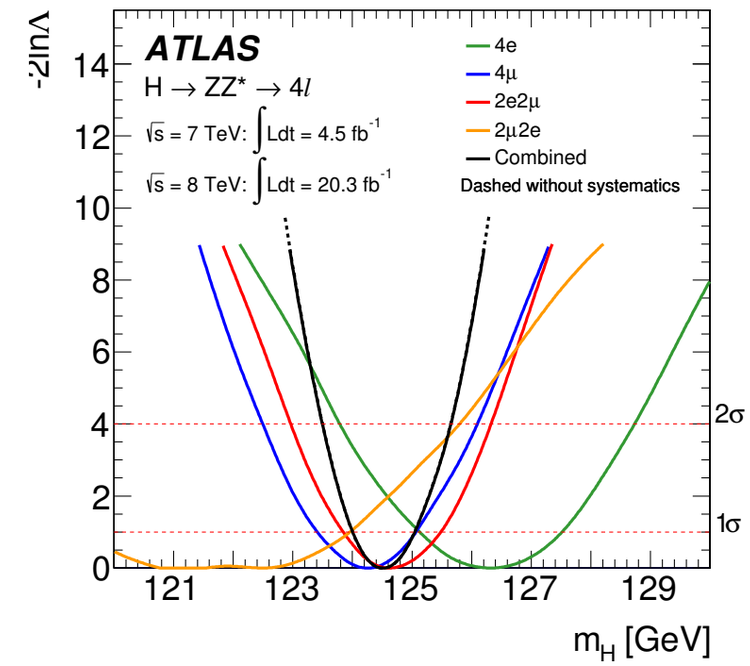

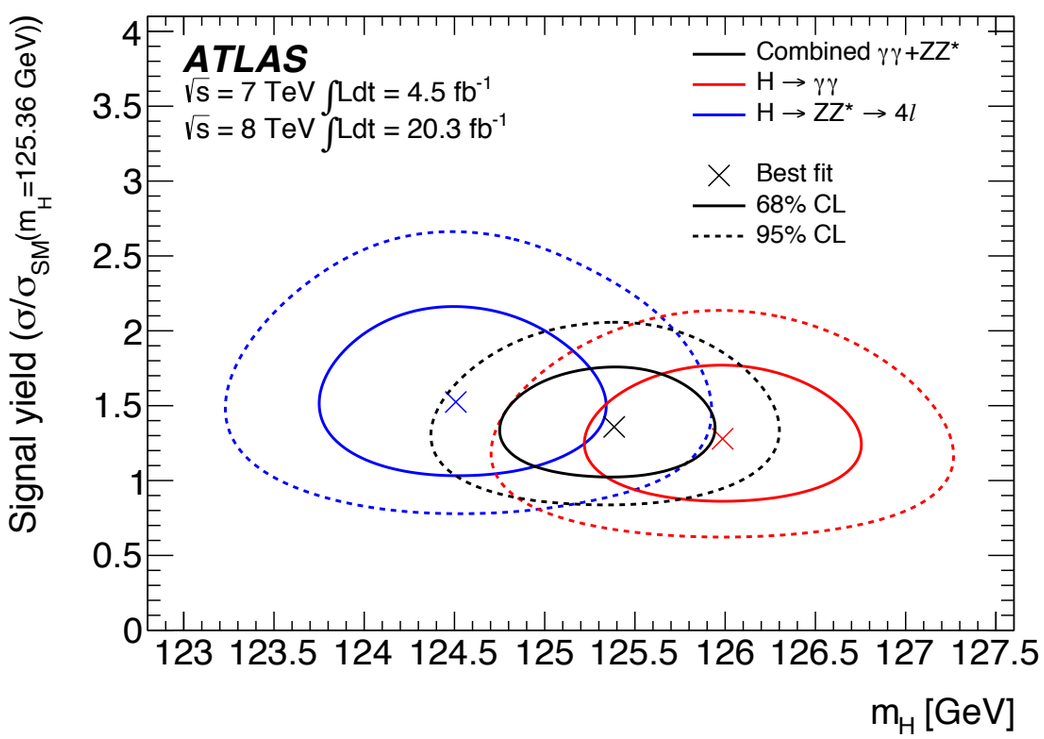

Channel	Mass measurement [GeV]
$H \to \gamma\gamma$	$125.98 \pm 0.42\,(\text{stat}) \pm 0.28\,(\text{syst}) = 125.98 \pm 0.50$
$H \to ZZ^* \to 4\ell$	$124.51 \pm 0.52\,(\text{stat}) \pm 0.06\,(\text{syst}) = 124.51 \pm 0.52$
Combined	$125.36 \pm 0.37\,(\text{stat}) \pm 0.18\,(\text{syst}) = 125.36 \pm 0.41$

0.3% precision!

Δm_H = 1.47±0.72 GeV compatible within 2σ

for details see Eleni's talk

Couplings Combination

arXiv:1507.04548

- measurements: H->WW, γγ, ZZ, ττ, bb
- limits: Zγ, μμ, ttH, off-shell (high mass)

$$\sigma_H(7\,\text{TeV}) = 22.1^{+7.4}_{-6.0}\,\text{pb}$$

$$\sigma_H(8\,\text{TeV}) = 27.7 \pm 3.7\,\text{pb}$$

$$\mu = 1.18^{+0.15}_{-0.14}$$

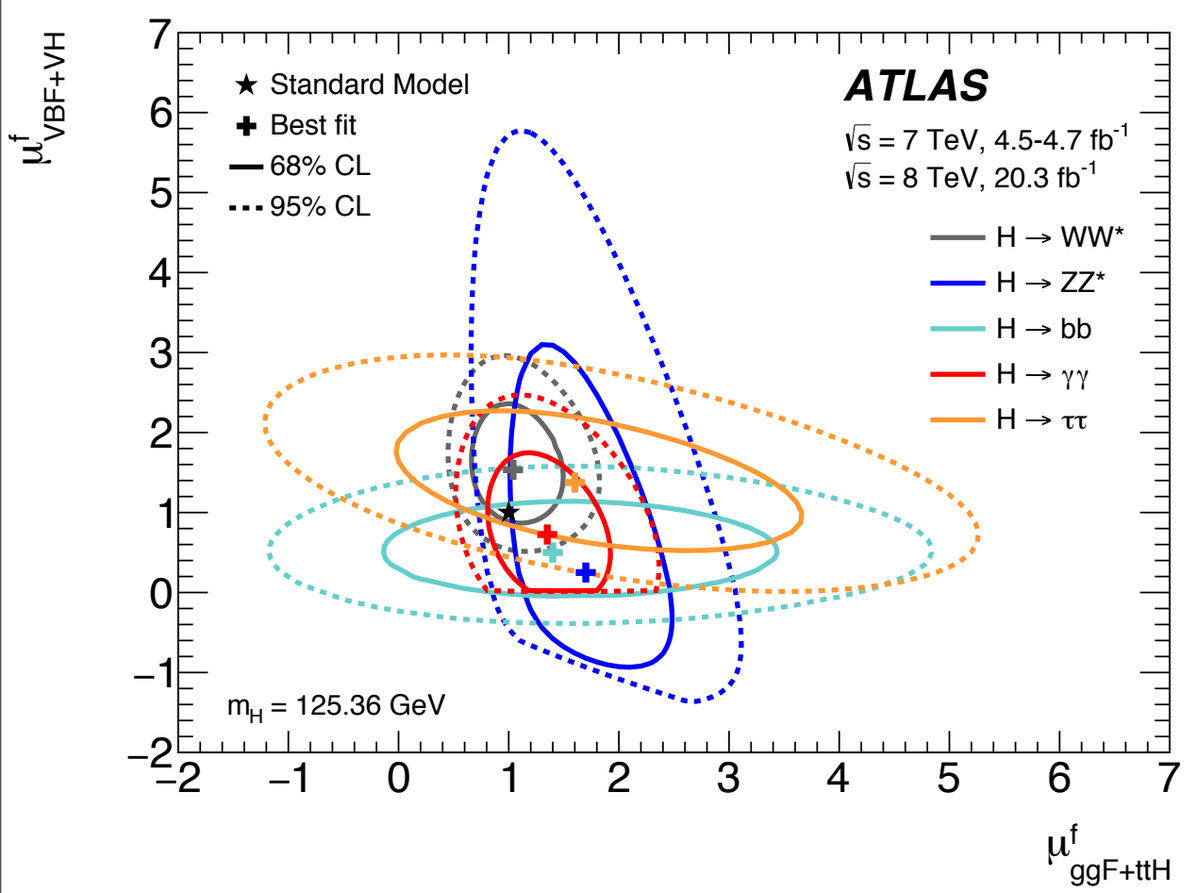

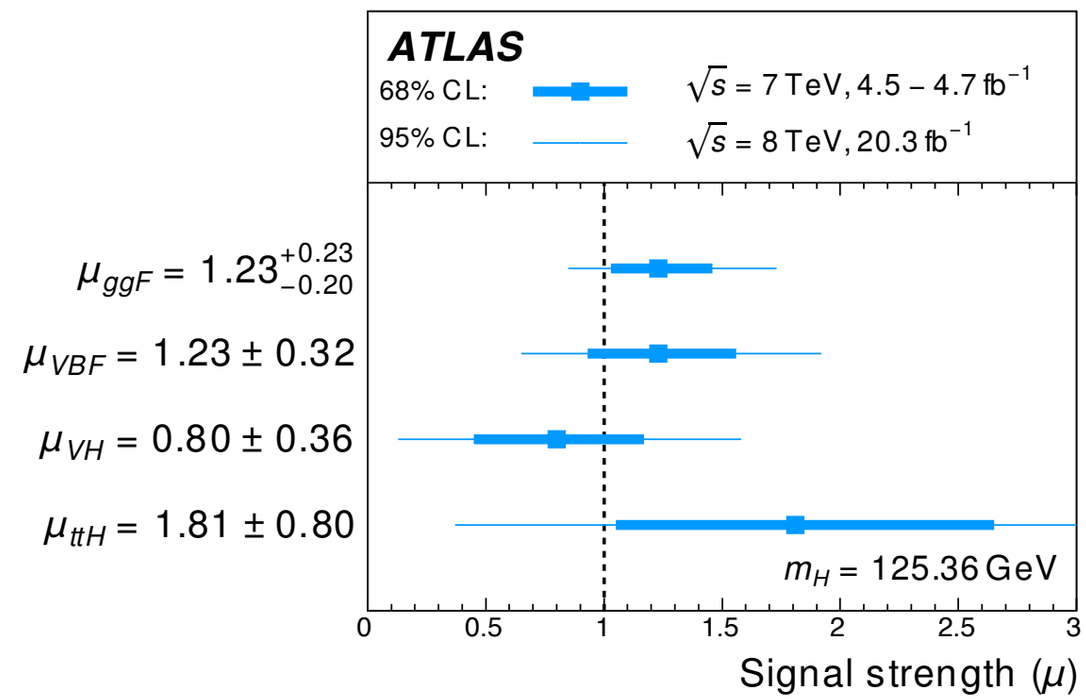

VBF 4.3σ, VH 2.6σ, ttH 2.3σ

The κ-framework

arXiv:1507.04548

- H: single, narrow resonance with m_H = 125.36 GeV
- decay kinematics compatible with SM
- tensor structure of interactions is the same
- zero-width approximation in the Higgs boson propagator, then:

$$\sigma(i \to H \to f) = \frac{\sigma_i(\kappa_j) \cdot \Gamma_f(\kappa_j)}{\Gamma_H(\kappa_j)}$$

  - parameter k represents deviation of coupling constants from SM (k = 1 <-> SM)

- **evidence for coupling to down-type fermions 4.5σ**

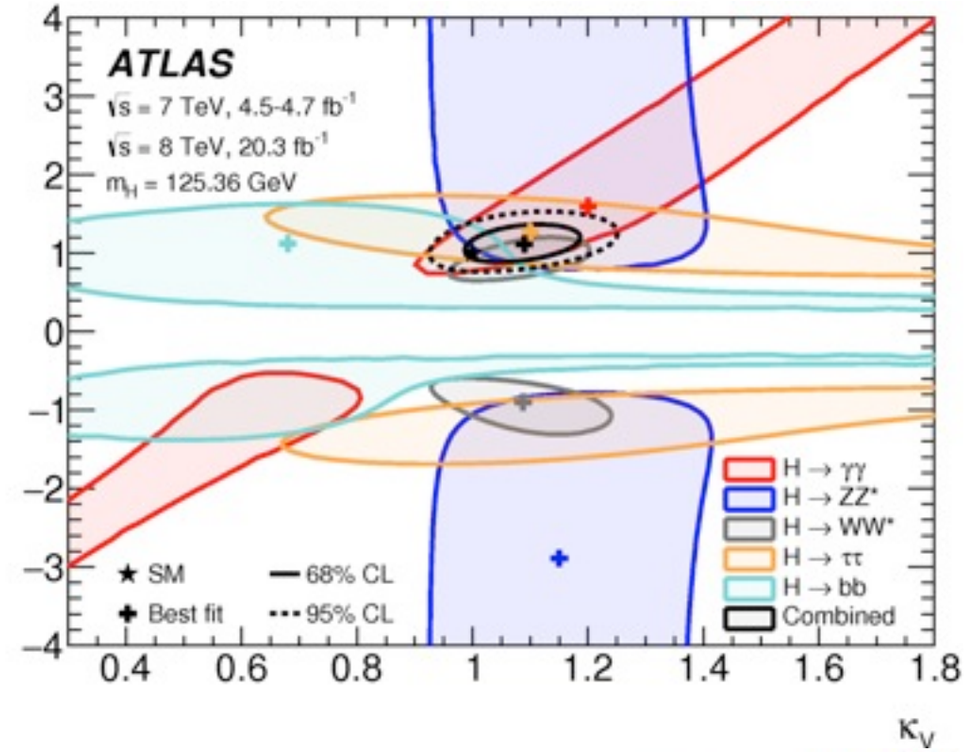

$$\kappa_V = \kappa_W = \kappa_Z \qquad \kappa_V = 1.09^{+0.07}_{-0.07}$$

$$\kappa_F = \kappa_t = \kappa_b = \kappa_\tau = \kappa_g = \kappa_\mu. \qquad \kappa_F = 1.11^{+0.17}_{-0.15}.$$

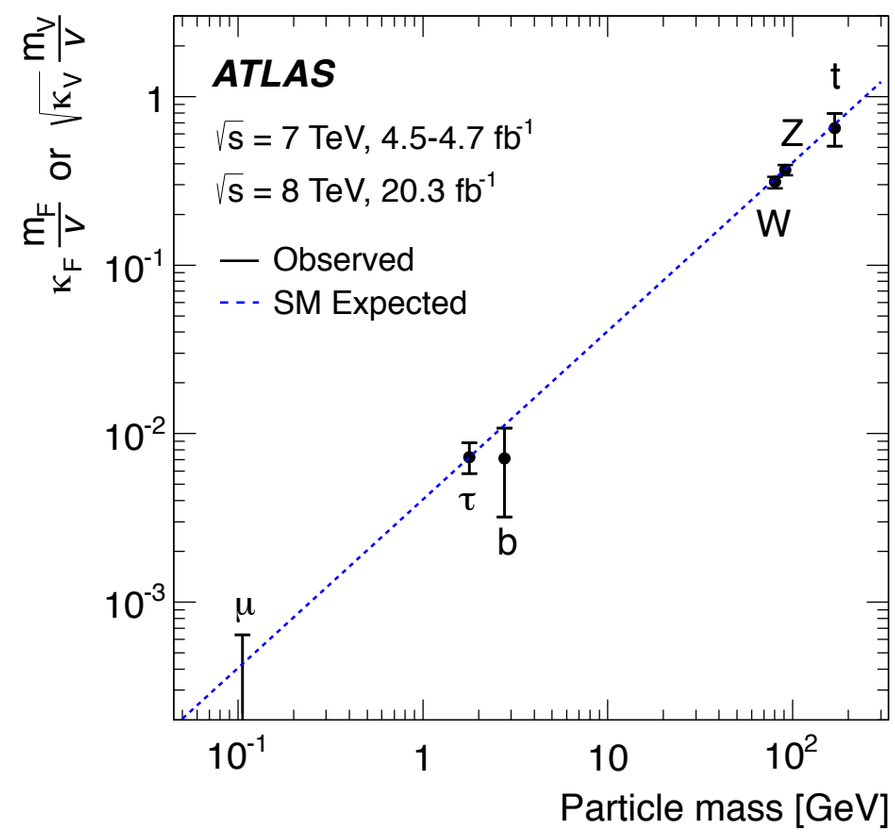

all κ independent

Spin & Parity

ATLAS-CONF-2015-008

- channels: ZZ, γγ and WW (eμ)
- **H->γγ:** spin-sensitive observables: $p_T^{\gamma\gamma}$, production of the two photons in Collins-Soper frame
  - 11 categories, fit on final yields
- **H->WW:** m_{ll}, p^T_{ll}, $\Delta\Phi_{ll}$ and m_T
  - 5 BDT trainings for different spins
- **H->4l:** angular variables of the leptons and planes
  - 4 categories based on lepton flavor
  - matrix element likelihood ratio analysis (MELA) and BDT
    - MELA: probability of observing a given event kinematics can be calculated -> discriminant
    - BDT: comparing hypotheses

H->γγ

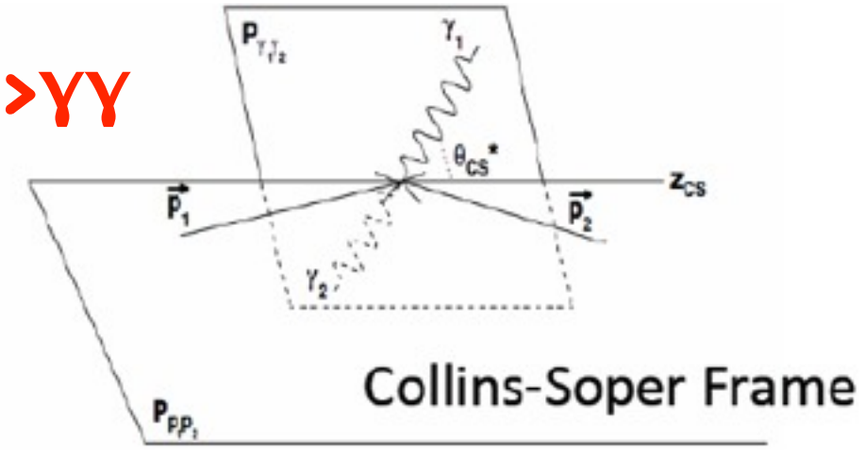

H->WW

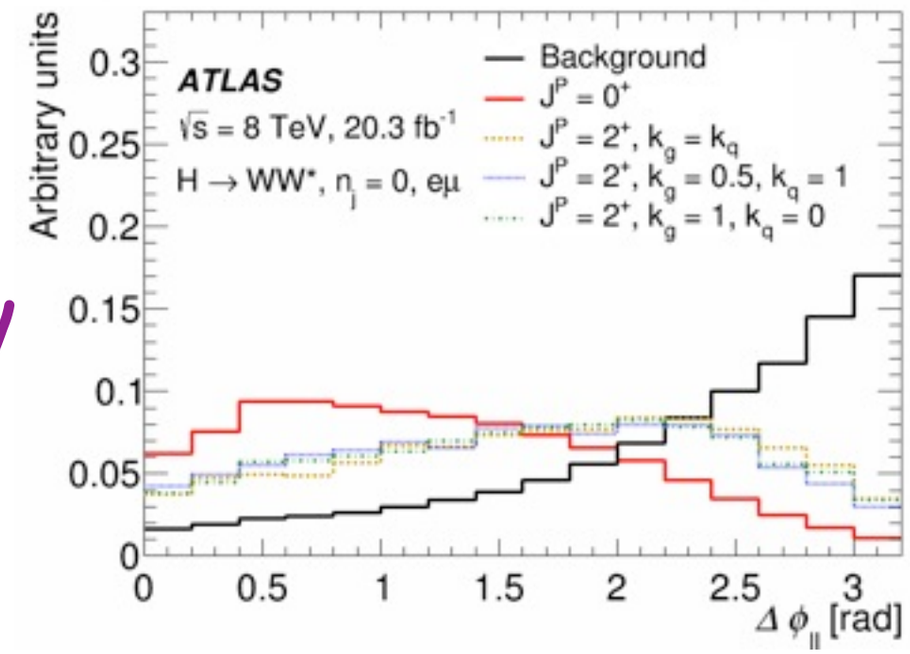

H->4l

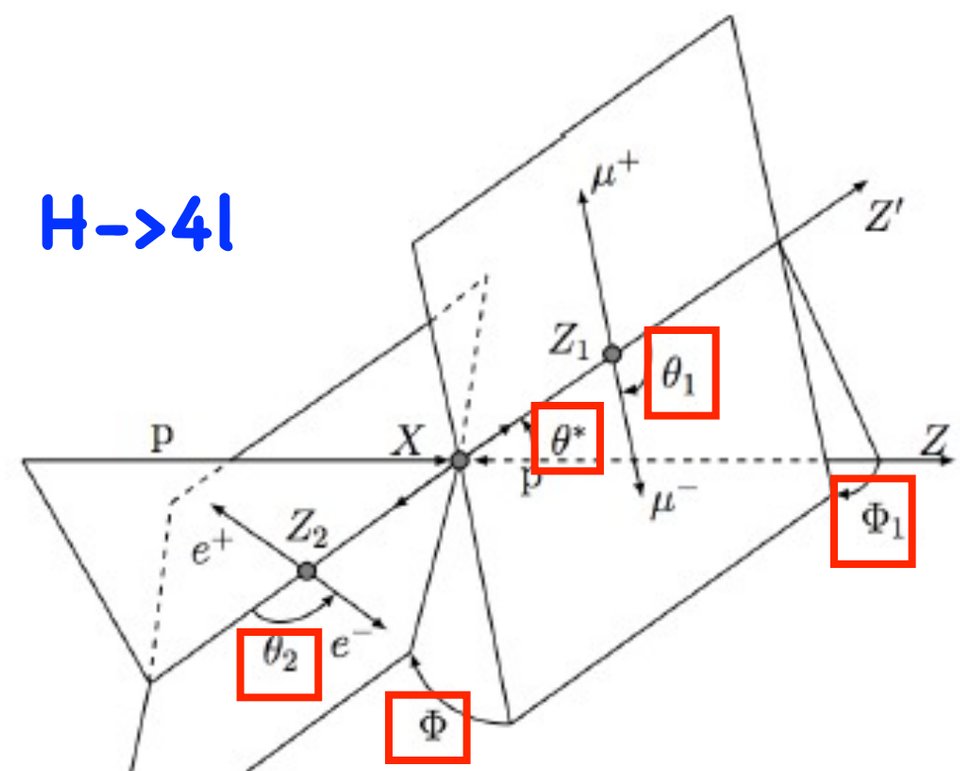

Spin & Parity

ATLAS-CONF-2015-008

- channels: ZZ, γγ and WW ($e\mu$)
- $J^P = 0^+$ is tested against other spin-0 models (0^-, BSM 0^+_h) and graviton-like $J^P = 2^+$
- also BSM terms in spin-0 are tested
- models rely on EFT, only H @ 125.4 GeV is considered
- valid up to Λ ~1TeV as minimum mass for BSM particles

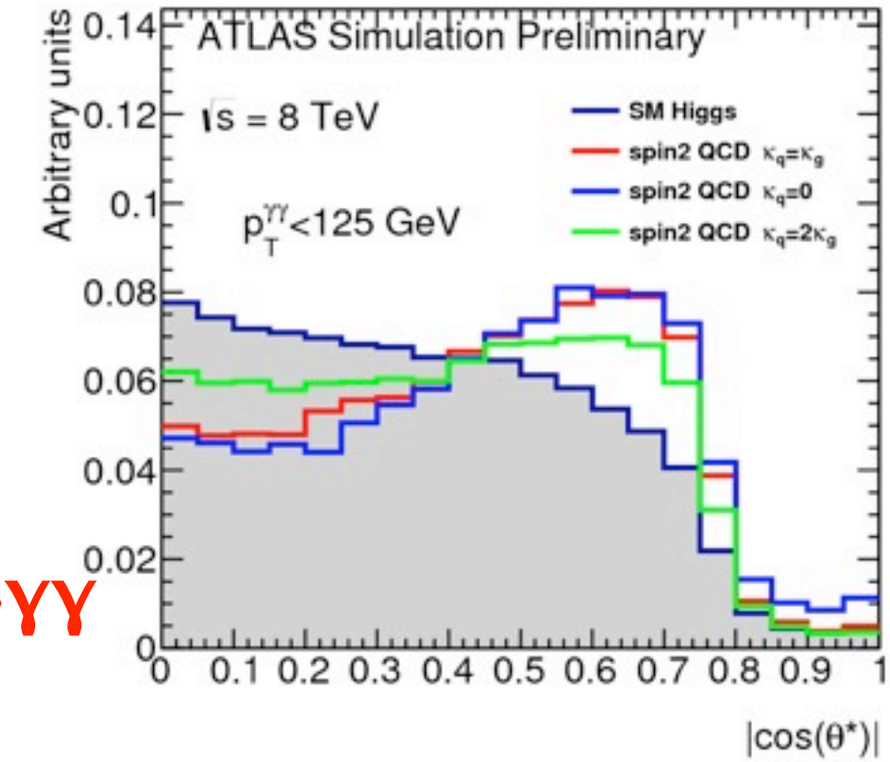

H->γγ

J^P	Model	Choice of tensor couplings			
		κ_{SM}	κ_{HVV}	κ_{AVV}	α
0^+	Standard Model Higgs boson	1	0	0	0
0^+_h	BSM spin-0 CP-even	0	1	0	0
0^-	BSM spin-0 CP-odd	0	0	1	$\pi/2$

$$\mathcal{L}_0^V = \Big\{ c_\alpha \kappa_{SM} \left[\tfrac{1}{2} g_{HZZ} Z_\mu Z^\mu + g_{HWW} W^+_\mu W^{-\mu} \right] - \frac{1}{4}\frac{1}{\Lambda} \left[c_\alpha \boxed{\kappa_{HZZ}} Z_{\mu\nu} Z^{\mu\nu} + s_\alpha \boxed{\kappa_{AZZ}} Z_{\mu\nu} \tilde{Z}^{\mu\nu} \right] - \frac{1}{2}\frac{1}{\Lambda} \left[c_\alpha \boxed{\kappa_{HWW}} W^+_{\mu\nu} W^{-\mu\nu} + s_\alpha \boxed{\kappa_{AWW}} W^+_{\mu\nu} \tilde{W}^{-\mu\nu} \right] \Big\} X_0$$

$\tilde{\kappa}_{HVV} \sim \kappa_{HVV}$

CP-even

CP-odd

Spin & Parity - Results

ATLAS-CONF-2015-008

- test statistic:

$$\mathcal{L}(\text{data} \mid J^P, \mu, \vec{\theta}) = \prod_j^{N_{\text{chann.}}} \prod_i^{N_{\text{bins}}} P(N_{i,j} \mid \mu_j \cdot S_{i,j}^{(J^P)}(\vec{\theta}) + B_{i,j}(\vec{\theta})) \times \mathcal{A}_j(\vec{\theta})$$

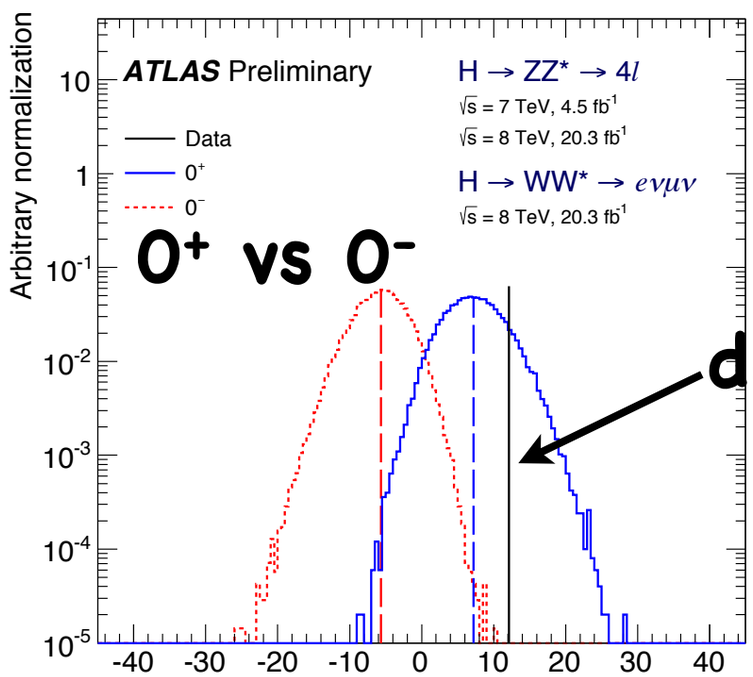

data

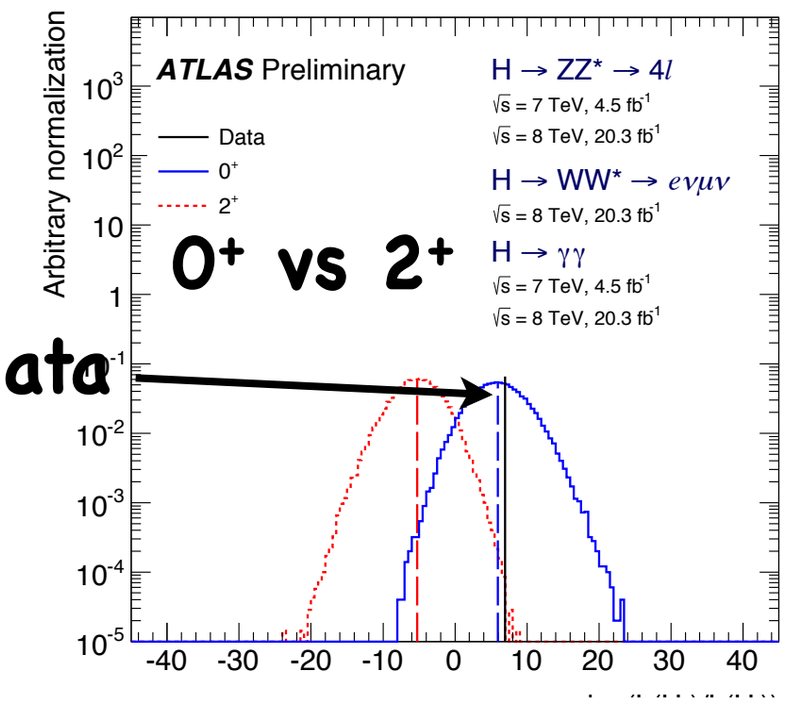

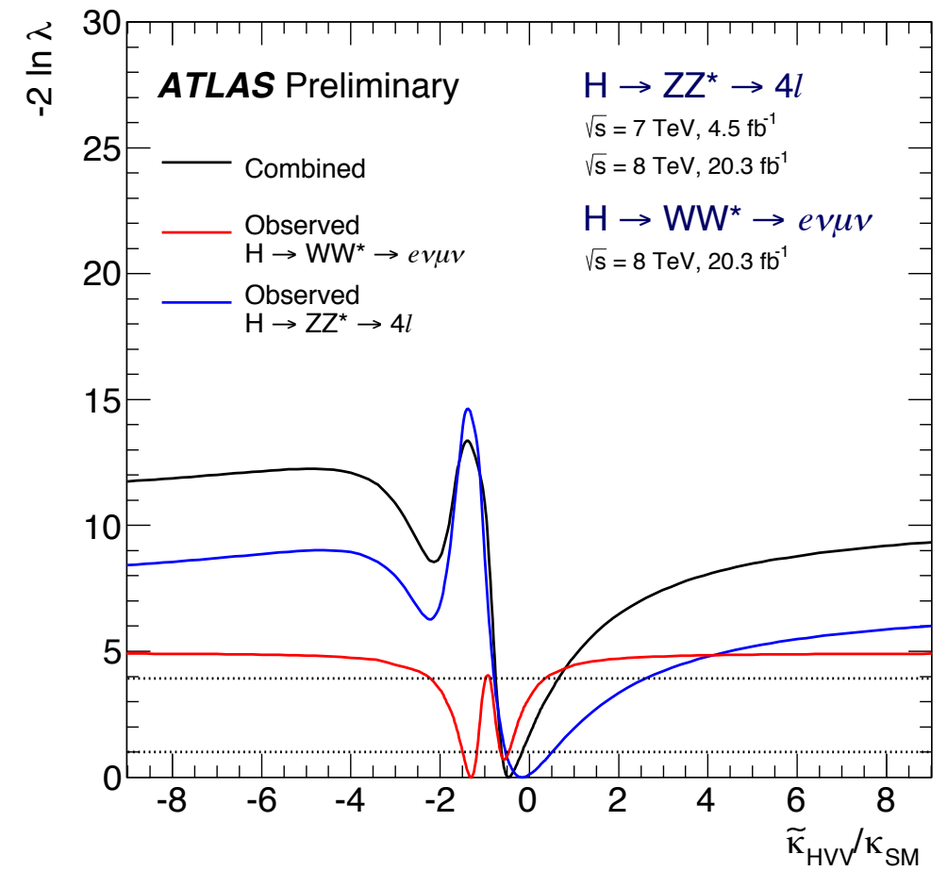

Coupling ratio	Best fit value		95% CL Exclusion Regions	
Combined	Expected	Observed	Expected	Observed
$\tilde{\kappa}_{HVV}/\kappa_{SM}$	0.0	−0.48	$(-\infty, -0.55] \bigcup [4.80, \infty)$	$(-\infty, -0.73] \bigcup [0.63, \infty)$
$(\tilde{\kappa}_{AVV}/\kappa_{SM}) \cdot \tan\alpha$	0.0	−0.68	$(-\infty, -2.33] \bigcup [2.30, \infty)$	$(-\infty, -2.18] \bigcup [0.83, \infty)$

exclusion of all non-SM spin models at more than 99% CL in favor of the 0+ hypothesis

ATLAS Run1 Higgs Legacy

$m_H = 125.36 \pm 0.41$ GeV

$\mu = 1.18^{+0.15}_{-0.14}$

$Z_0(VFB) = 4.3\sigma$

$Z_0(VH) = 2.6\sigma$

$Z_0(ttH) = 2.2\sigma$

evidence for down-type coupling to fermions = 4.5σ

in the most flexible coupling model, coupling precision is 15-40%

exclusion of all non-SM spin models at more than 99% CL in favor of the 0^+ hypothesis

backup

ATLAS @ LHC

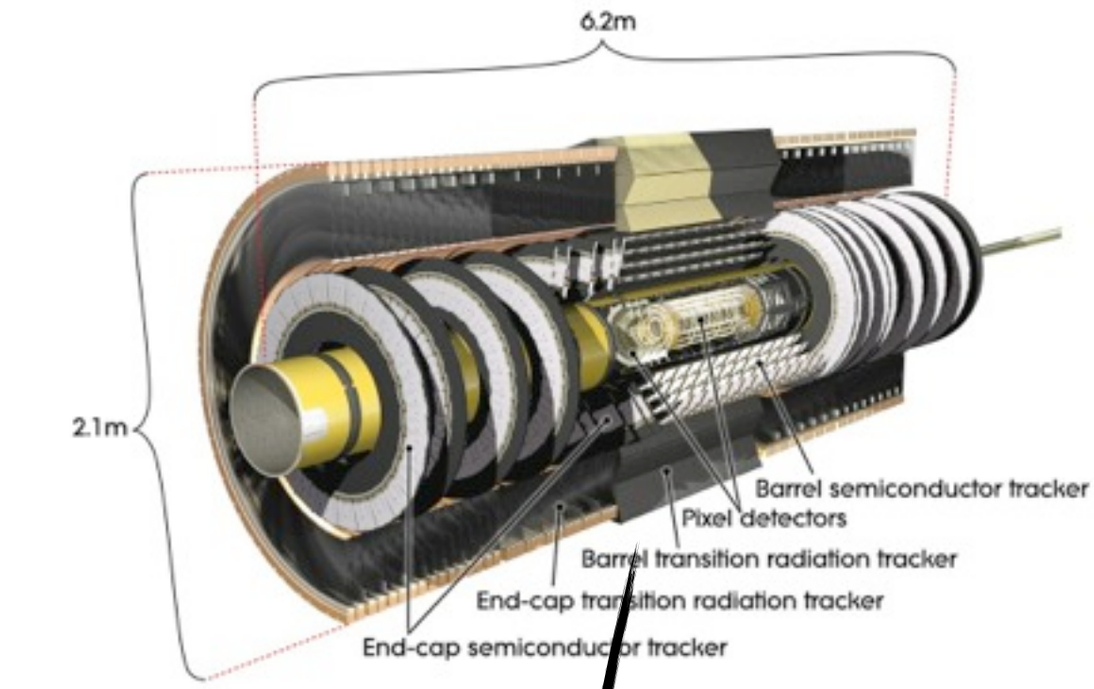

- 4π detector, 44x25m, 7000t
- ID (PIX, SCT, TRT) -> solenoid magnet (2T) -> Calo (LAr - EM, TileCal/LAr - Had) -> toroid magnets (4T) -> muon system (MDT, CSC, RPC, TGC)

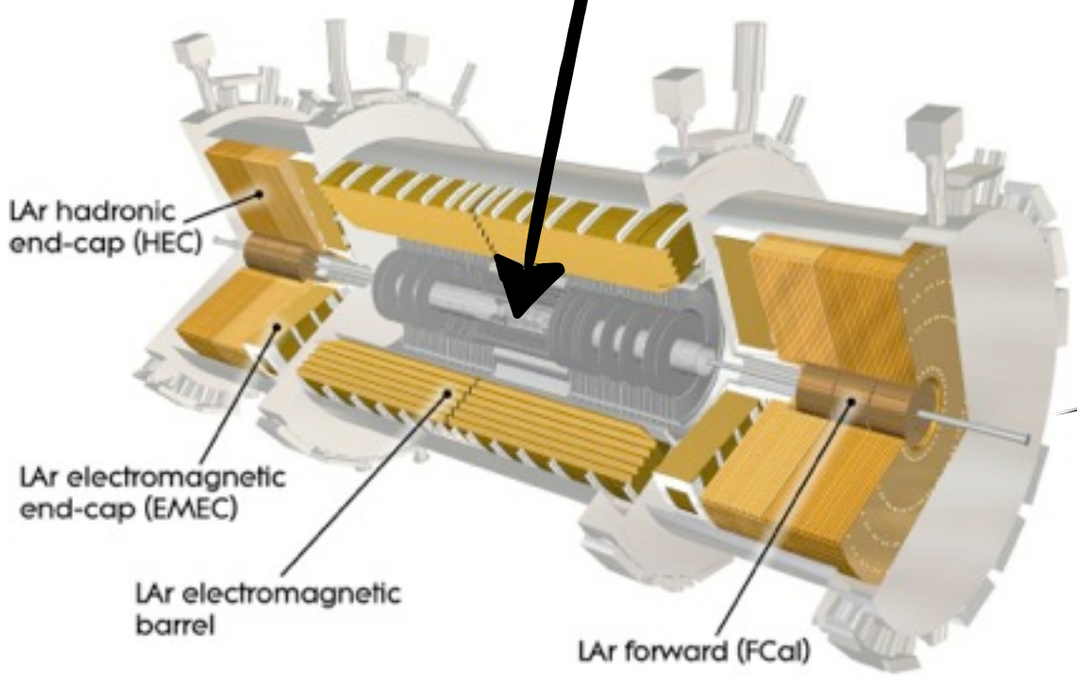

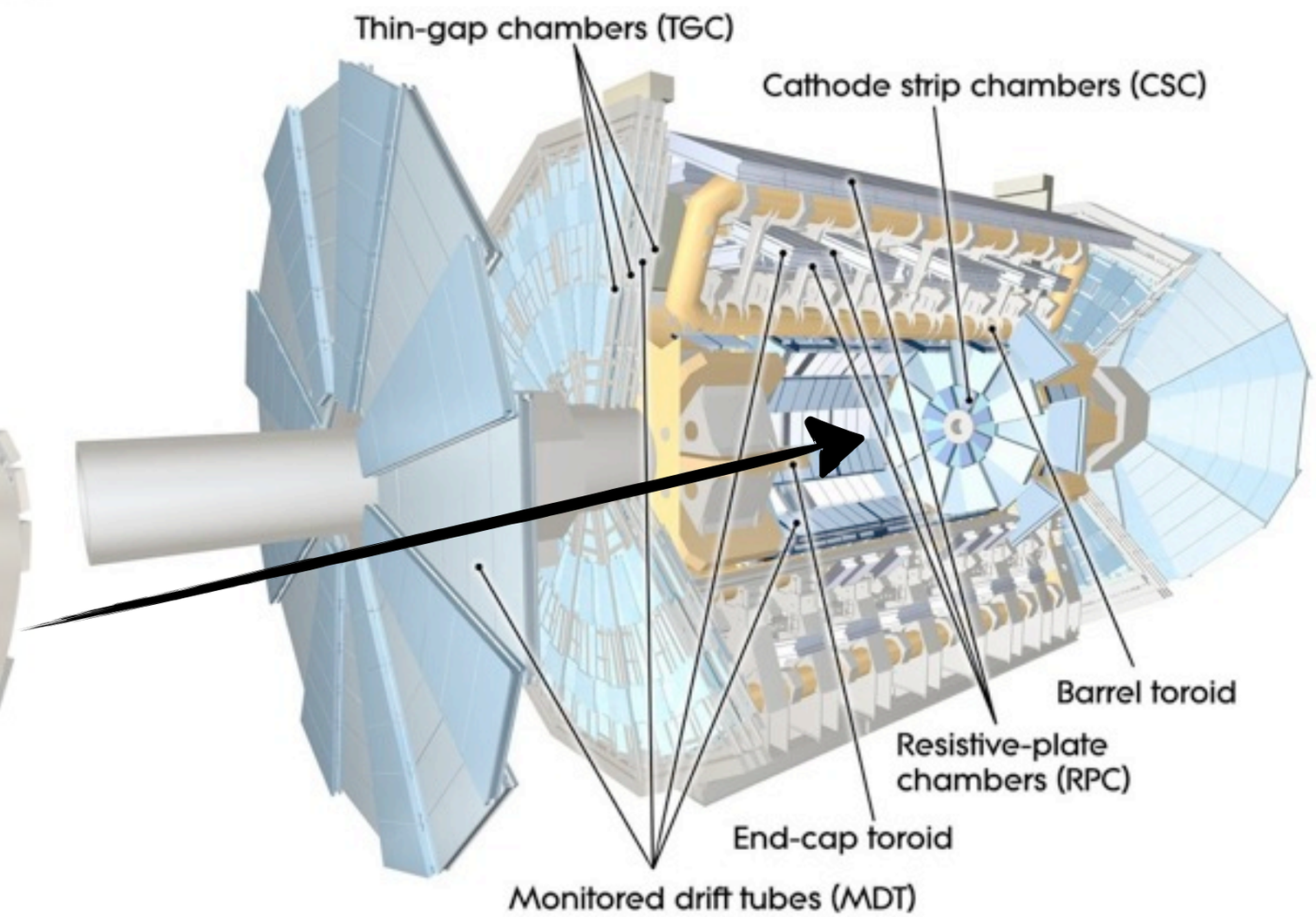

mass combination

Table 4: Principal systematic uncertainties on the combined mass. Each uncertainty is determined from the change in the 68% CL range for m_H when the corresponding nuisance parameter is removed (fixed to its best fit value), and is calculated by subtracting this reduced uncertainty from the original uncertainty in quadrature.

Systematic	Uncertainty on m_H [MeV]
LAr syst on material before presampler (barrel)	70
LAr syst on material after presampler (barrel)	20
LAr cell non-linearity (layer 2)	60
LAr cell non-linearity (layer 1)	30
LAr layer calibration (barrel)	50
Lateral shower shape (conv)	50
Lateral shower shape (unconv)	40
Presampler energy scale (barrel)	20
ID material model ($\|\eta\| < 1.1$)	50
$H \to \gamma\gamma$ background model (unconv rest low p_{Tt})	40
$Z \to ee$ calibration	50
Primary vertex effect on mass scale	20
Muon momentum scale	10
Remaining systematic uncertainties	70
Total	180

coupling inputs

Table 2: Overview of the individual analyses that are included in the combinations described in this paper. The signal strengths, the statistical significances of a Higgs boson signal, or the 95% CL upper limits on the Higgs boson production rates or properties are also shown wherever appropriate. A range is quoted for the upper limit on the off-shell signal strength, depending on the assumption of the continuum $gg \to WW/ZZ$ cross section. These results are taken directly from individual publications. Results of the on-shell analyses are quoted for $m_H = 125.36$ GeV except that $m_H = 125.5$ GeV is assumed for the $H \to Z\gamma$ and $H \to \mu\mu$ analyses and that $m_H = 125$ GeV is used for the ttH searches with $H \to b\bar{b}$ and $ttH \to$ multileptons. The luminosity used for the $\sqrt{s} = 7$ TeV $VH \to Vb\bar{b}$ analysis differs slightly from the other analyses because a previous version of the luminosity calibration was applied. The significance is given in units of standard deviations (σ). The numbers in parentheses are the expected values from the SM Higgs boson. The ttH analysis in the $H \to \gamma\gamma$ decay is part of the $H \to \gamma\gamma$ analysis and is also included separately under the ttH production for completeness. The checkmark (✓) indicates whether the analysis is performed for the respective $\sqrt{s} = 7$ and 8 TeV dataset.

Analysis	Signal		$\int \mathcal{L}dt$ (fb^{-1})	
Categorisation or final states	Strength	Significance [σ]	7 TeV	8 TeV
$H \to \gamma\gamma$ [12]	1.17 ± 0.27	5.2 (4.6)	4.5	20.3
ttH: leptonic, hadronic			✓	✓
VH: one-lepton, dilepton, E_T^{miss}, hadronic			✓	✓
VBF: tight, loose			✓	✓
ggF: 4 p_{Tt} categories			✓	✓
$H \to ZZ^* \to 4\ell$ [13]	$1.44^{+0.40}_{-0.33}$	8.1 (6.2)	4.5	20.3
VBF			✓	✓
VH: hadronic, leptonic			✓	✓
ggF			✓	✓
$H \to WW^*$ [14, 15]	$1.16^{+0.24}_{-0.21}$	6.5 (5.9)	4.5	20.3
ggF: (0-jet, 1-jet) $\otimes$ ($ee + \mu\mu$, $e\mu$)			✓	✓
ggF: $\geq$ 2-jet and $e\mu$				✓
VBF: $\geq$ 2-jet $\otimes$ ($ee + \mu\mu$, $e\mu$)			✓	✓
VH: opposite-charge dilepton, three-lepton, four-lepton			✓	✓
VH: same-charge dilepton				✓
$H \to \tau\tau$ [17]	$1.43^{+0.43}_{-0.37}$	4.5 (3.4)	4.5	20.3
Boosted: $\tau_{lep}\tau_{lep}, \tau_{lep}\tau_{had}, \tau_{had}\tau_{had}$			✓	✓
VBF: $\tau_{lep}\tau_{lep}, \tau_{lep}\tau_{had}, \tau_{had}\tau_{had}$			✓	✓
$VH \to Vb\bar{b}$ [18]	0.52 ± 0.40	1.4 (2.6)	4.7	20.3
0ℓ ($ZH \to \nu\nu bb$): $N_{jet} = 2, 3$, $N_{btag} = 1, 2$, $p_T^V >$ and < 120 GeV			✓	✓
1ℓ ($WH \to \ell\nu bb$): $N_{jet} = 2, 3$, $N_{btag} = 1, 2$, $p_T^V >$ and < 120 GeV			✓	✓
2ℓ ($ZH \to \ell\ell bb$): $N_{jet} = 2, 3$, $N_{btag} = 1, 2$, $p_T^V >$ and < 120 GeV			✓	✓

coupling inputs

Table 2: Overview of the individual analyses that are included in the combinations described in this paper. The signal strengths, the statistical significances of a Higgs boson signal, or the 95% CL upper limits on the Higgs boson production rates or properties are also shown wherever appropriate. A range is quoted for the upper limit on the off-shell signal strength, depending on the assumption of the continuum $gg \to WW/ZZ$ cross section. These results are taken directly from individual publications. Results of the on-shell analyses are quoted for $m_H = 125.36$ GeV except that $m_H = 125.5$ GeV is assumed for the $H \to Z\gamma$ and $H \to \mu\mu$ analyses and that $m_H = 125$ GeV is used for the ttH searches with $H \to b\bar{b}$ and $ttH \to$ multileptons. The luminosity used for the $\sqrt{s} = 7$ TeV $VH \to Vb\bar{b}$ analysis differs slightly from the other analyses because a previous version of the luminosity calibration was applied. The significance is given in units of standard deviations (σ). The numbers in parentheses are the expected values from the SM Higgs boson. The ttH analysis in the $H \to \gamma\gamma$ decay is part of the $H \to \gamma\gamma$ analysis and is also included separately under the ttH production for completeness. The checkmark (✓) indicates whether the analysis is performed for the respective $\sqrt{s} = 7$ and 8 TeV dataset.

	95% CL limit		
$H \to Z\gamma$ [19]	$\mu < 11$ (9)	4.5	20.3
10 categories based on $\Delta\eta_{Z\gamma}$ and p_{Tt}		✓	✓
$H \to \mu\mu$ [20]	$\mu < 7.0$ (7.2)	4.5	20.3
VBF and 6 other categories based on η_μ and $p_{\mathrm{T}}^{\mu\mu}$		✓	✓
ttH production [21–23]		4.5	20.3
$H \to b\bar{b}$: single-lepton, dilepton	$\mu < 3.4$ (2.2)		✓
$ttH \to$multileptons: categories on lepton multiplicity	$\mu < 4.7$ (2.4)		✓
$H \to \gamma\gamma$: leptonic, hadronic	$\mu < 6.7$ (4.9)	✓	✓
Off-shell H^* production [24]	$\mu < 5.1 - 8.6$ (6.7 – 11.0)		20.3
$H^* \to ZZ \to 4\ell$			✓
$H^* \to ZZ \to 2\ell 2\nu$			✓
$H^* \to WW \to e\nu\mu\nu$			✓

kappa fwk

Table 6: Overview of Higgs boson production cross sections σ_i and Higgs boson partial decay widths Γ_f. For each production or decay mode the scaling of the corresponding rate in terms of Higgs boson coupling strength scale factors is given. For processes where multiple amplitudes contribute, the rate may depend on multiple Higgs boson coupling strength scale factors, and interference terms may give rise to scalar product terms $\kappa_i\kappa_j$ that allow to determine the relative sign of the coupling strengths κ_i and κ_j. Expressions originate from Ref. [11], except for $\sigma(gg \to ZH)$ (from Ref. [40]) and $\sigma(gb \to WtH)$ and $\sigma(qb \to tHq')$ (calculated using Ref. [26]). The expressions are given for $\sqrt{s} = 8$ TeV and $m_H = 125.36$ GeV and are similar for $\sqrt{s} = 7$ TeV. Interference contributions with negligible magnitudes have been been omitted in this table.

Production	Loops	Interference	Expression in terms of fundamental coupling strengths
$\sigma(\mathrm{ggF})$	✓	$b-t$	$\kappa_g^2 \sim 1.06 \cdot \kappa_t^2 + 0.01 \cdot \kappa_b^2 - 0.07 \cdot \kappa_t\kappa_b$
$\sigma(\mathrm{VBF})$	-	-	$\sim 0.74 \cdot \kappa_W^2 + 0.26 \cdot \kappa_Z^2$
$\sigma(WH)$	-	-	$\sim \kappa_W^2$
$\sigma(q\bar{q} \to ZH)$	-	-	$\sim \kappa_Z^2$
$\sigma(gg \to ZH)$	✓	$Z-t$	$\kappa_{ggZH}^2 \sim 2.27 \cdot \kappa_Z^2 + 0.37 \cdot \kappa_t^2 - 1.64 \cdot \kappa_Z\kappa_t$
$\sigma(bbH)$	-	-	$\sim \kappa_b^2$
$\sigma(ttH)$	-	-	$\sim \kappa_t^2$
$\sigma(gb \to WtH)$	-	$W-t$	$\sim 1.84 \cdot \kappa_t^2 + 1.57 \cdot \kappa_W^2 - 2.41 \cdot \kappa_t\kappa_W$
$\sigma(qb \to tHq')$	-	$W-t$	$\sim 3.4 \cdot \kappa_t^2 + 3.56 \cdot \kappa_W^2 - 5.96 \cdot \kappa_t\kappa_W$
Partial decay width			
$\Gamma_{b\bar{b}}$	-	-	$\sim \kappa_b^2$
Γ_{WW}	-	-	$\sim \kappa_W^2$
Γ_{ZZ}	-	-	$\sim \kappa_Z^2$
$\Gamma_{\tau\tau}$	-	-	$\sim \kappa_\tau^2$
$\Gamma_{\mu\mu}$	-	-	$\sim \kappa_\mu^2$
$\Gamma_{\gamma\gamma}$	✓	$W-t$	$\kappa_\gamma^2 \sim 1.59 \cdot \kappa_W^2 + 0.07 \cdot \kappa_t^2 - 0.66 \cdot \kappa_W\kappa_t$
$\Gamma_{Z\gamma}$	✓	$W-t$	$\kappa_{Z\gamma}^2 \sim 1.12 \cdot \kappa_W^2 + 0.00035 \cdot \kappa_t^2 - 0.12 \cdot \kappa_W\kappa_t$
Total decay width			
Γ_H	✓	$W-t$ $b-t$	$\kappa_H^2 \sim 0.57 \cdot \kappa_b^2 + 0.22 \cdot \kappa_W^2 + 0.09 \cdot \kappa_g^2 + 0.06 \cdot \kappa_\tau^2 + 0.03 \cdot \kappa_Z^2 + 0.03 \cdot \kappa_c^2 + 0.0023 \cdot \kappa_\gamma^2 + 0.0016 \cdot \kappa_{Z\gamma}^2 + 0.00022 \cdot \kappa_\mu^2$

kappa fwk

Table 7: Summary of coupling benchmark models considered in this paper, where $\lambda_{ij} \equiv \kappa_i/\kappa_j$, $\kappa_{ii} \equiv \kappa_i\kappa_i/\kappa_H$, and the functional dependence assumptions are: $\kappa_V = \kappa_W = \kappa_Z$, $\kappa_F = \kappa_t = \kappa_b = \kappa_\tau = \kappa_\mu$ (and similarly for the other fermions), $\kappa_g = \kappa_g(\kappa_b, \kappa_t)$, $\kappa_\gamma = \kappa_\gamma(\kappa_b, \kappa_t, \kappa_\tau, \kappa_W)$, and $\kappa_H = \kappa_H(\kappa_i)$. The tick marks indicate which assumptions are made in each case. The last column shows, as an example, the relative coupling strengths involved in the $gg \to H \to \gamma\gamma$ process.

Section in this paper	Corresponding table in [11]	Probed couplings	Parameters of interest	Functional assumptions					Example: $gg \to H \to \gamma\gamma$
				κ_V	κ_F	κ_g	κ_γ	κ_H	
5.2.1	43.1	Couplings to fermions and bosons	κ_V, κ_F	✓	✓	✓	✓	✓	$\kappa_F^2 \cdot \kappa_\gamma^2(\kappa_F, \kappa_V)/\kappa_H^2(\kappa_F, \kappa_V)$
5.2.2	43.3		$\lambda_{FV}, \kappa_{VV}$	✓	✓	✓	✓	–	$\kappa_{VV}^2 \cdot \lambda_{FV}^2 \cdot \kappa_\gamma^2(\lambda_{FV}, \lambda_{FV}, \lambda_{FV}, 1)$
5.3.1	48.1	Vertex loops + H→invisible/undetected decays	$\kappa_g, \kappa_\gamma, \kappa_{Z\gamma}$	=1	=1	–	–	✓	$\kappa_g^2 \cdot \kappa_\gamma^2/\kappa_H^2(\kappa_g, \kappa_\gamma)$
5.3.2	48.2		$\kappa_g, \kappa_\gamma, \kappa_{Z\gamma}, BR_{i.,u.}$	=1	=1	–	–	✓	$\kappa_g^2 \cdot \kappa_\gamma^2/\kappa_H^2(\kappa_g, \kappa_\gamma) \cdot (1 - BR_{i.,u.})$
5.4.1	43.2		$\kappa_F, \kappa_V, BR_{i.,u.}$	≤ 1	–	✓	✓	✓	$\frac{\kappa_F^2 \cdot \kappa_\gamma(\kappa_F, \kappa_V)^2}{\kappa_H^2(\kappa_F, \kappa_V)} \cdot (1 - BR_{i.,u.})$
				–	–	✓	✓	μ_{off}	
5.4.2	49		$\kappa_F, \kappa_V, \kappa_g, \kappa_\gamma, \kappa_{Z\gamma}, BR_{i.,u.}$	≤ 1	–	–	–	✓	$\frac{\kappa_F^2 \cdot \kappa_\gamma(\kappa_F, \kappa_V)^2}{\kappa_H^2(\kappa_F, \kappa_V, \kappa_g, \kappa_\gamma)} \cdot (1 - BR_{i.,u.})$
				–	–	–	–	μ_{off}	
5.5.1	46	Up-/down-type fermions	$\lambda_{du}, \lambda_{Vu}, \kappa_{uu}$	✓	κ_u, κ_d	✓	✓	–	$\kappa_{uu}^2 \cdot \kappa_g^2(\lambda_{du}, 1) \cdot \kappa_\gamma^2(\lambda_{du}, 1, \lambda_{du}, \lambda_{Vu})$
5.5.2	47	Leptons/quarks	$\lambda_{lq}, \lambda_{Vq}, \kappa_{qq}$	✓	κ_l, κ_q	✓	✓	–	$\kappa_{qq}^2 \cdot \kappa_\gamma^2(1, 1, \lambda_{lq}, \lambda_{Vq})$
5.6.1	51	Generic models with and without assumptions on vertex loops and Γ_H	$\kappa_W, \kappa_Z, \kappa_t, \kappa_b, \kappa_\tau, \kappa_\mu$	–	–	✓	✓	✓	$\frac{\kappa_g^2(\kappa_b, \kappa_t) \cdot \kappa_\gamma^2(\kappa_b, \kappa_t, \kappa_\tau, \kappa_\mu, \kappa_W)}{\kappa_H^2(\kappa_b, \kappa_t, \kappa_\tau, \kappa_\mu, \kappa_W, \kappa_Z)}$
5.6.2	50.2		$\kappa_W, \kappa_Z, \kappa_t, \kappa_b, \kappa_\tau, \kappa_\mu, \kappa_g, \kappa_\gamma, \kappa_{Z\gamma}, BR_{i.,u.}$	≤ 1	–	–	–	✓	$\frac{\kappa_g^2 \cdot \kappa_\gamma^2}{\kappa_H^2(\kappa_b, \kappa_t, \kappa_\tau, \kappa_\mu, \kappa_W, \kappa_Z)} \cdot (1 - BR_{i.,u.})$
				–	–	–	–	✓	
				–	–	–	–	μ_{off}	
5.6.3	50.3		$\lambda_{WZ}, \lambda_{tg}, \lambda_{bZ}, \lambda_{\tau Z}, \lambda_{gZ}, \lambda_{\gamma Z}, \lambda_{Z\gamma Z}, \kappa_{gZ}$ $\kappa_{gZ}, \lambda_{Z\gamma Z}$	–	–	–	–	–	$\kappa_{gZ}^2 \cdot \lambda_{\gamma Z}^2$

most generic model

- allows deviations in vertex loop couplings strengths, no assumption on the total width

$$\kappa_{gZ} = \kappa_g \cdot \kappa_Z / \kappa_H$$
$$\lambda_{Zg} = \kappa_Z / \kappa_g$$
$$\lambda_{WZ} = \kappa_W / \kappa_Z$$
$$\lambda_{tg} = \kappa_t / \kappa_g$$
$$\lambda_{bZ} = \kappa_b / \kappa_Z$$
$$\lambda_{\tau Z} = \kappa_\tau / \kappa_Z$$
$$\lambda_{\mu Z} = \kappa_\mu / \kappa_Z$$
$$\lambda_{\gamma Z} = \kappa_\gamma / \kappa_Z$$
$$\lambda_{(Z\gamma)Z} = \kappa_{Z\gamma} / \kappa_Z .$$

- precision 15%-40%

Parameter		Measurement
κ_{gZ}	=	1.18 ± 0.16
λ_{Zg}	=	$1.09^{+0.26}_{-0.22}$
λ_{WZ}	$\in$	$[-1.04, -0.81] \cup [0.80, 1.06]$
λ_{tg}	$\in$	$[-1.70, -1.07] \cup [1.03, 1.73]$
λ_{bZ}	=	0.60 ± 0.27
$\lambda_{\tau Z}$	=	$0.99^{+0.23}_{-0.19}$
$\lvert\lambda_{\mu Z}\rvert$	<	2.3 (95% CL)
$\lambda_{\gamma Z}$	=	0.90 ± 0.15
$\lvert\lambda_{(Z\gamma)Z}\rvert$	<	3.2 (95% CL)

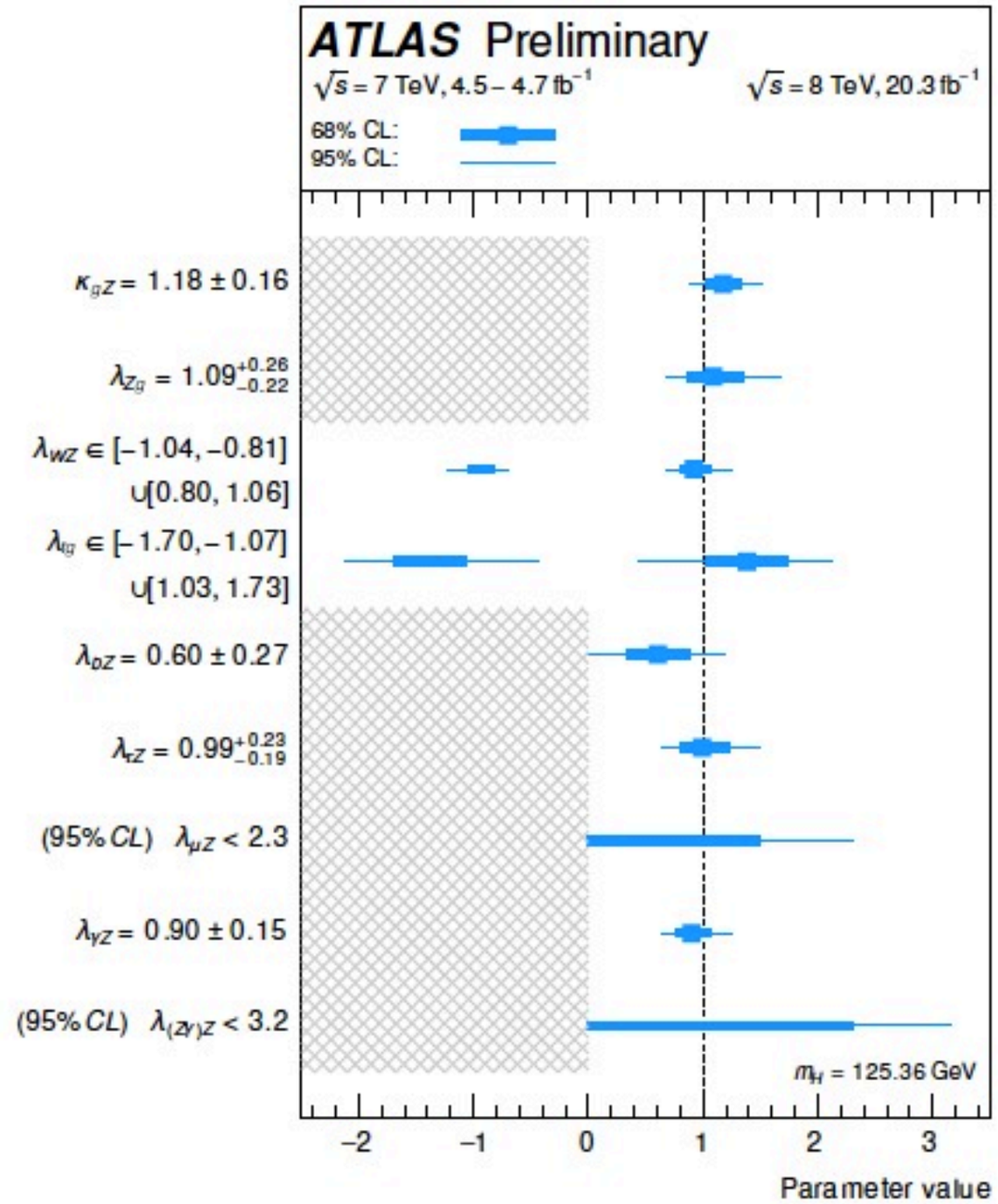

Collins-Soper frame

The kinematic variables sensitive to the spin of the resonance are the diphoton transverse momentum $p_{\mathrm{T}}^{\gamma\gamma}$ and the production angle of the two photons, measured in the Collins-Soper frame [31]:

$$|\cos\theta^*| = \frac{|\sinh(\Delta\eta^{\gamma\gamma})|}{\sqrt{1+(p_{\mathrm{T}}^{\gamma\gamma}/m_{\gamma\gamma})^2}}\frac{2p_{\mathrm{T}}^{\gamma 1}p_{\mathrm{T}}^{\gamma 2}}{m_{\gamma\gamma}^2}, \tag{7}$$

where $\Delta\eta^{\gamma\gamma}$ is the separation in pseudo-rapidity of the two photons.

H->4l, MELA

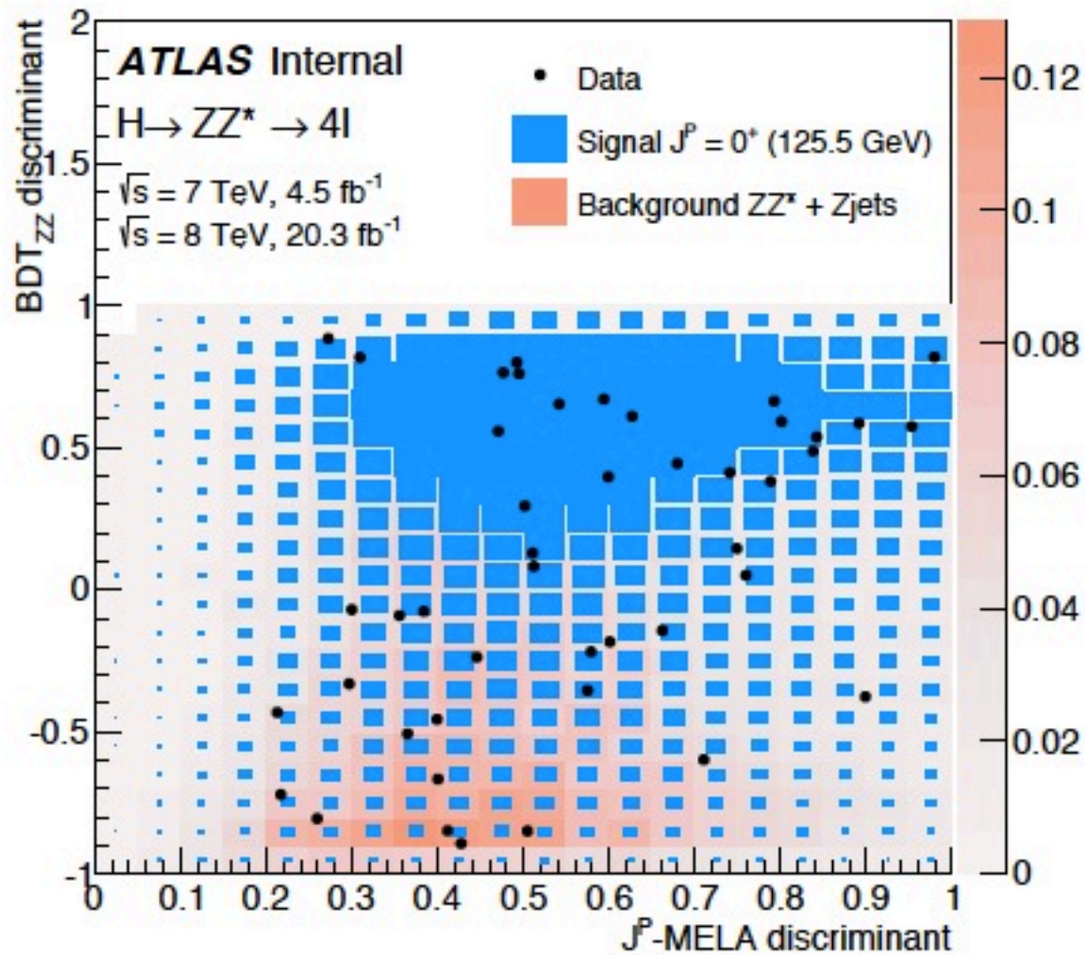

Figure 5: The distributions of the background discriminant $\mathrm{BDT_{ZZ}}$ versus the J^P – MELA discriminant for the $J^P = 0^+$ and $J^P = 0^-$ signal hypotheses in the signal region 115 GeV $< m_{4\ell} <$ 130 GeV.